

We are IntechOpen, the world's leading publisher of Open Access books Built by scientists, for scientists

4,800

Open access books available

122,000

International authors and editors

135M

Downloads

Our authors are among the

154

Countries delivered to

TOP 1%

most cited scientists

12.2%

Contributors from top 500 universities



WEB OF SCIENCE™

Selection of our books indexed in the Book Citation Index
in Web of Science™ Core Collection (BKCI)

Interested in publishing with us?
Contact book.department@intechopen.com

Numbers displayed above are based on latest data collected.

For more information visit www.intechopen.com



CFD Simulations of Crude Oil Fouling on Heat Transfer Surfaces

Ramasamy Marappa Gounder and Sampath Emani

Additional information is available at the end of the chapter

<http://dx.doi.org/10.5772/intechopen.71886>

Abstract

Advancements in the computational techniques have led to the development of various numerical models and methods to predict the occurrence of crude oil fouling in heat exchangers. Computational fluid dynamics has been employed in the field of crude oil fouling research in the recent past, which led to the concept of investigating the effects of various operating conditions on deposit formations on heat transfer surfaces. Various processes associated with crude oil fouling, such as asphaltenes precipitation and chemical reactions, have been studied through CFD simulations. This chapter provides state-of-the-art review on various CFD approaches and describes the discrete-phase CFD modeling of crude oil fouling through asphaltenes deposition on heat transfer surfaces.

Keywords: crude oil, fouling, discrete phase, CFD, heat transfer

1. Introduction

Crude oil is one of the major fossil fuels/energy resources in today's world. Crude oil consists of a complex mixture of hydrocarbons with various molecular weights which are distilled into various fractions in refineries. The crude oil is normally preheated by recovering heat in a battery of preheat exchangers from the separated fractions and pump-around flows from crude distillation unit. Efficient recovery of heat from the product streams is very essential to minimize the specific energy requirement of processing the crude oil as nearly 6% of the total energy content of each barrel of crude oil is used in the refinery itself.

The deposition of unwanted materials on heat transfer surfaces is termed as fouling. The heat exchangers in the crude preheat trains are highly prone to fouling due to the presence of solid particles and components that precipitate as solid particles upon heating the crude oils. Fouling in the crude preheat train leads to several consequences in the refineries. Efficient recovery of heat in the heat exchangers and the delicate balance of heat integration suffer a major blow due

to the fouling in heat exchangers. The foulant deposits, with much lower thermal conductivities than that of the tube metal, reduce the heat transfer coefficients and eventually result in decreased energy recovery. When the extent of fouling reaches the limits of operation either in the furnace that provides the additional heat necessary or in the pumping capacity due to the increased pressure drops, a plant shutdown becomes necessary for cleaning the heat exchangers and restoring their heat transfer efficiencies. Furthermore, crude oil fouling has also a high impact on the environment. It has been observed that about 2.5% of the worldwide environmental pollution emissions are caused due to fouling [1]. Crude oil fouling involves production losses during planned and unplanned shutdowns for cleaning and high costs for cleaning and associated activities. The total cost of fouling in various refineries has been estimated to be approximately \$1.5 billion per year globally [2].

Fouling process is a physicochemical phenomenon and its mechanisms have been classified into the following five types: particulate (sedimentation) fouling; chemical reaction fouling; corrosion fouling; crystallization fouling; and biological fouling. Particulate fouling is described as the deposition of dirt, clay, or rust suspended in the fluid onto the heat transfer surface [3]. The deposition resulting from one or more chemical reactions between the components contained in the fluid is termed as chemical reaction fouling [4, 5]. When the deposition is the result of a chemical reaction that involves a component in the fluid and the metal surface, it is called as corrosion fouling [6]. Corrosion fouling usually results in a rough surface and creates new sites for fouling. The precipitation of dissolved salts in the saturated solutions due to their solubility changes with temperature and deposition on the heat transfer surfaces is known as crystallization fouling [6]. Biological fouling is the formation of organic films consisting of microorganisms that promote attachment of microorganisms, such as mussels, algae, etc., [7]. Crude oil fouling in refineries can occur by any of the mechanisms described above except the biological fouling. Irrespective of the fouling mechanism, the last steps of the fouling process, in general, are the transportation and/or deposition of solid particles on the heat transfer surfaces.

The crude oil fouling mitigation techniques, generally in practice, are frequent cleaning of heat exchangers, use of chemical additives, i.e., anti-foulants, operation under threshold fouling conditions and use of physical methods such as modified tube bundles with helical baffles, coated tubes, twisted tubes, and tube inserts. Operations at or under the threshold fouling conditions will ensure zero or minimum fouling. Threshold fouling conditions are normally specified by operating regimes of high flow velocities and low film temperatures. The uncertainties involved in establishing the effectiveness of fouling mitigation techniques in refineries have led to the development of various fouling simulation and predictive models.

Various empirical, semi-empirical, and fundamental fouling models have been proposed to study the crude oil fouling phenomenon [8–12]. Most of the fouling models in literature predict fouling rates based on the operating conditions and fluid properties and the models do not include the mathematical descriptions of fluid flow and heat transfer processes. Computational fluid dynamics, on the other hand, provides an opportunity to model fluid flow and heat transfer behaviors along with the fouling phenomenon simultaneously. Even though, the physical and chemical phenomena involved in fouling processes are highly complex, the overall understanding of the fouling behavior and its mechanisms were enhanced from the past few decades with various CFD models [13–16].

In general, shell and tube heat exchanger design assumes that fluid flow through the bundle of tubes is evenly distributed. Practical experience has shown that this is not always true and the consequences of maldistribution in terms of poor performance and increased fouling are often severe [17]. Uneven distribution of fluid flow means areas of low velocity and vortex formation within the tube bundle leading to areas of ineffective heat transfer and increased risk of tube side fouling. Computational fluid dynamics has not often been used to investigate the crude oil fouling phenomena in shell and tube heat exchangers. Studies on shell-side crude oil fouling in shell and tube heat exchangers have been reported in literature, which neglected the tube side fluid flow [18–20]. An arbitrary fixed linear temperature profile on the tube wall was assumed to investigate the shell side fouling which neglects the thermal interactions between tube and shell-side fluids. These studies have demonstrated that fouling is more prone to happen near the inlet and baffle openings due to low velocity zones.

In this chapter, an attempt has been made to review the various CFD models for predicting the crude oil fouling phenomena. Section 2 presents the fouling studies using CFD modeling and effects of operating conditions on fouling. Section 3 presents the CFD simulations of asphaltenes deposition in a heat exchanger tube through Discrete Phase Model (DPM). A summary of present trend in employing CFD to crude oil fouling and future developments will be discussed in Section 4.

2. Computational fluid dynamics and fouling modeling

2.1. Introduction to CFD

Computational fluid dynamics is one of the branches of fluid dynamics that uses numerical methods and algorithms to solve and analyze various fluid flow problems [21]. It gives an insight into flow patterns that are difficult, expensive, or impossible to study using experimental techniques. Its applications in a wide variety of disciplines in process industries have led to a reduction in the need for physical experimentations.

Being time-dependent in nature, fouling is a process that should be monitored continuously in time. As such, fouling experiments are time-consuming and often difficult to perform. In view of the above, CFD has been used as one of the predominant approaches to investigate crude oil fouling phenomena. The crude oil fouling process involves momentum transfer, mass transfer, heat transfer, flow turbulence, and chemical reactions. Detailed CFD models describing the fouling processes are often very complex to solve numerically and requires simplifications for reducing the computational load. The fluid-flow is generally governed by incompressible Navier-Stokes equations for mass, momentum and energy as given in Eqs. (1)–(3).

Continuity equation:

$$\frac{\partial \rho}{\partial t} + \nabla \cdot (\rho \bar{v}) = 0 \quad (1)$$

Momentum equation:

$$\frac{\partial(\overline{\rho v})}{\partial t} + \nabla \cdot (\overline{\rho v v}) = -\nabla p + \nabla \cdot (\overline{\tau}) + \rho \overline{g} \quad (2)$$

Energy equation:

$$\frac{\partial(\rho C_p T)}{\partial t} + \nabla \cdot (\rho C_p \vec{v} T) = \nabla \cdot (k \Delta T) + H \quad (3)$$

Fouling mechanisms are generally associated with turbulent flows, mainly due to the higher fluid velocities and complex geometry of heat exchangers. The turbulent flow condition is the chaotic and random state of fluid motion, associated with disturbances in the fluid streamlines of laminar flows [22]. Turbulent flow plays a significant role in various fluid dynamic applications and its modeling has undergone intensive research. The simulation of turbulent flow using Navier-Stokes equations is possible through direct numerical simulations (DNS) model, which requires a huge amount of computational time and memory. Due to the limitations in the computational capabilities, the basic conservative equations such as mass, momentum and energy are unable to resolve the fluid motion associated with turbulent flow regimes [23]. Therefore, most of the cases involving turbulent flows are solved through Reynolds-averaged Navier Stokes (RANS) equations which are developed by adapting suitable time-averaging techniques on Navier-Stokes equations. Several turbulence models such as k - ϵ , k - ω , Reynolds Stress Model (RSM), etc., are available within the RANS equations to approximate the influence of turbulent fluctuations in the flow domain. In k - ϵ turbulence model, the energy in the turbulence is computed from the turbulent kinetic energy (k) and the rate of dissipation of the turbulent kinetic energy is computed from the turbulent dissipation (ϵ). The k - ω turbulence model predicts turbulence with turbulence kinetic energy (k) with a specific rate of dissipation (ω). Reynolds Stress Model is a higher-level turbulence model which is considered for predicting the complex interactions in the turbulence flow fields. The most common turbulence model considered in the field of crude oil fouling is k - ϵ model [13, 24–28], which assumes that the turbulence is isotropic and requires less computational time for simulation.

The turbulent kinetic energy, k is described by:

$$\frac{\partial k}{\partial t} + (v_i \cdot \nabla)k - \nabla \cdot \left(\frac{\mu_t}{\sigma_k} \nabla \cdot k \right) = P^k - \epsilon + S_k \quad (4)$$

and dissipation rate, ϵ (epsilon) is given by:

$$\frac{\partial \epsilon}{\partial t} + (v_i \cdot \nabla)\epsilon - \nabla \cdot \left(\frac{\mu_t}{\sigma_\epsilon} \nabla \epsilon \right) = \frac{\epsilon}{k} (C_1 P^k - C_2 \epsilon) + S_\epsilon \quad (5)$$

The k - ω turbulence model was also considered in a few crude oil fouling CFD studies [14, 16, 29]. It is found to be numerically stable and is reported to achieve precise simulation results in comparison with other models [16, 30].

Specific dissipation rate, ω (omega) used in the k - ω turbulence model is given by:

$$(\bar{\nu} \cdot \nabla) \omega = \nabla \cdot [(\mu + \mu_T \sigma_\omega) \nabla \omega] + \alpha \frac{\omega}{k} P_k - \beta_0 \omega^2 \quad (6)$$

2.2. Fouling modeling

Fouling can occur either through a series of reactions and/or without any reactions. The deposition process associated with fouling is studied through CFD simulations by two routes, viz.: (i) asphaltene deposition fouling and (ii) chemical reaction fouling [13, 31, 32].

2.2.1. Asphaltene deposition fouling

Asphaltene constituents are categorized as the most polar and highest molecular weight fraction of petroleum [26, 33] and are considered as the heaviest component in the crude oil [34]. Asphaltenes tend to precipitate and deposit on heat transfer surfaces [35] under changes in pressure and temperature conditions. The probability of the precipitated asphaltene particles ending up as foulant deposits on the heat transfer surface depends on various forces acting on the particles such as inertial, gravity, drag, Saffman lift, buoyancy, thermophoretic, etc. Particles in high fluid velocity regions have higher inertial forces and the probabilities of particles reaching the heat transfer surface and rebound or splash are high and, therefore, cause less fouling. At high temperature gradients near the surface, the thermophoretic forces predominate the other forces acting on the particles and favor the particles to stick to the surface as foulant particles.

Several CFD models that capture some or all the above forces were developed to understand the fouling phenomena associated with asphaltene particles in the crude oil [13, 15, 16, 29, 31, 32, 36–38]. The CFD models employed were classified into Eulerian-Eulerian and Eulerian-Lagrangian models based on how the solids phase is treated. The Eulerian-Eulerian model treats the particles as a continuum and applies the governing equations in a similar approach as that for the fluid phase [39], while the Eulerian-Lagrangian method treats the particles as a discrete phase and the pathway of individual particles are tracked [39, 40].

2.2.1.1. Eulerian-Eulerian model

Multiphase fluids are modeled in CFD by three different Eulerian-Eulerian multiphase models, viz.: (i) Volume-of-Fluid (VOF) model, (ii) mixture model, and (iii) Eulerian model. Volume-of-Fluid model is desirable for the studies in which the interface between two or more immiscible fluids is of interest [26]. Mixture model is mostly considered for simulating the particle-laden flows, bubbly flow regimes, etc. The basic assumption in the mixture model is that all the phases share the same turbulence field [41]. Eulerian model is the most complex model compared with VoF and mixture models and is used for simulating bubble columns, particle suspension and fluidized beds.

In Eulerian-Eulerian models, the components of the crude oils are categorized into two phases, viz.: (i) non-asphaltenes and (ii) asphaltenes. The non-asphaltenes phase of the crude oil is assumed as the primary phase, while the asphaltenes are considered as the secondary phase

[13, 32]. In order to understand the fluid flow behavior and asphaltenes deposition in the system, one of the Eulerian-Eulerian multiphase models can be chosen. Volume-of-Fluid multiphase model is highly used for predicting the asphaltenes deposition on the heat transfer surfaces [13, 26, 31]. The deposition profile of asphaltenes is predicted from the volume fraction contours. The interface tracking between the phases is governed by the solution of a continuity equation for the volume fraction of multiphases. For q^{th} phase, interface tracking is computed as:

$$\frac{\partial}{\partial t}(\rho Y_i) + \nabla \cdot (\rho Y_i \bar{v}) = -\nabla \cdot \bar{J}_i + R_i + S_i \quad (7)$$

2.2.1.2. Eulerian-Lagrangian approach

The Eulerian-Lagrangian model treats the asphaltene particles as a discrete phase, in which, the model tracks the trajectory of the individual particles. The crude oil, which is the primary phase, is considered as a continuum on which the governing equations are computed. Asphaltene particles present in the crude oil are partly in the colloidal form and partly in dissolved form. The asphaltene particles precipitated from the crude oil might be carried forward with the flow without causing any fouling [42] while some of the asphaltene particles may get deposited on heat transfer surface due to various attractive/repulsive forces [43]. Several forces, such as gravity, drag, Saffman lift, buoyancy, Brownian diffusion, and thermophoretic, act on the asphaltene particles [37].

The trajectory of the asphaltene particles inside the heat exchanger tube is calculated by:

$$\frac{dv_p}{dt} = F_D(v - v_p) + \frac{g_i(\rho_p - \rho)}{\rho_p} + F_i \quad (8)$$

The particles drag force is estimated as:

$$F_D = \frac{18\mu C_D \text{Re}}{\rho_p d_p^2 24} \quad (9)$$

where

$$C_D = \frac{24}{\text{Re}}(1 + b_1 \text{Re}^{b_2}) + \frac{b^3 \text{Re}}{b_4 + \text{Re}} \quad (10)$$

$$\text{Re} = \frac{\rho d_p |v_p - v|}{\mu} \quad (11)$$

The thermophoretic force is computed by [44]:

$$F_{th} = -D_{T,p} \frac{1}{m_p T} \frac{\partial T}{\partial x} \quad (12)$$

where the thermophoretic force coefficient, $D_{T,p}$ is given by:

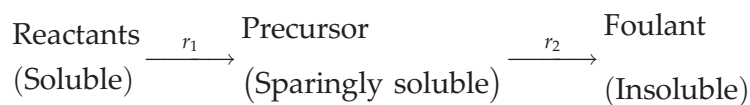
$$D_{T,p} = \frac{\mu^2 C_s \left(\left(\frac{k}{k_p} \right) + C_t Kn \right)}{\rho \left(1 + 3C_m Kn \right) \left(1 + 2 \left(\frac{k}{k_p} \right) + 2C_t Kn \right)} \quad (13)$$

The magnitude of the shear-induced lift force on particles is computed using Saffman equation [45]:

$$\vec{F} = \frac{2Kv^{1/2} \rho d_{ij}}{\rho_p d_p (d_{ik} d_{kl})^{1/4}} (\vec{v} - \vec{v}_p) \quad (14)$$

2.2.2. Chemical reaction fouling

Chemical reaction fouling has been identified as the main cause of crude oil fouling on the heat transfer surfaces. A highly complex chemical kinetic scheme is involved in chemical reaction fouling route, in which, the intermediate species are formed via various elementary reactions. Various CFD studies investigated the coke formation due to the chemical reactions in the bulk and/or surface through species transport model [13, 14, 16, 25, 26, 46]. The components of crude oil such as, asphaltenes, salt, resins, etc., were added as species to bulk flow (crude oil). The basic assumption considered in the current chemical reaction models is that the chemical reaction fouling route involves a two-step reaction process [32], namely, initial generation of soluble precursors and formation of insoluble foulant particles, as



where r_1 and r_2 are the reaction rates given by:

$$r_1 = k_1 c_{r,1}^m c_{r,2}^n \quad (15)$$

$$r_2 = k_2 c_p^l \quad (16)$$

and k_1 and k_2 are the reaction rate constants specified by the Arrhenius equation:

$$k_i = A \exp \left(\frac{-E}{RT} \right) \quad (17)$$

The CFD methodology involved in predicting the foulant mass through chemical reaction fouling route involves a three-step process. Initially, crude oil fluid flow without the foulant species is simulated in the heat exchanger. Subsequently, the foulant species are introduced in the fully developed fluid flow. The reactions of the species are defined on the tube surface to observe the formation of fouling layer. Petroleum is considered as the bulk fluid and the coke content is specified at the inlet as zero [13, 14].

2.3. Effect of operating conditions

2.3.1. Flow velocity

The flow velocity has a high significance on the deposition rate of fouling precursors from the crude oil. Asphaltene particles suspended from the crude oil will deposit on the heat transfer surface under low-velocity conditions. An increase in the flow velocity is expected to promote the dislodging of asphaltene particles deposited on the surface through increased shear stress [13, 16]. The inertial forces on the particles in high fluid velocity regions will be high. Thus, the probabilities of particles reaching the heat transfer surface and causing rebound or splash events are high and, therefore, cause less fouling. The irregular flow profiles, reverse flow paths, and low-velocity regions in the domain can be visualized through CFD study. Various CFD studies reported that fouling rate reduces with an increase in flow velocity [16, 29, 32]. The mass depositions of asphaltenes and coke on the heat transfer surface were observed to reduce gradually with increase in the Reynolds number [24, 25, 32]. Fouling resistance on the heat transfer surface was predicted at different flow velocities ranging from 0.05 to 0.2 m/s and observed that at higher velocities the fouling resistance decreases [47].

2.3.2. Temperature difference between the bulk-fluid and wall

Crude oil fouling is highly dependent on the temperature difference, ΔT , between the bulk-fluid and wall. Various CFD studies reported that with the decrease in temperature difference, the deposit formation reduces [13, 16, 27]. The reason behind the reduced deposition is because of the thermophoretic effect acting on the fouling precursors. Even though, a few experimental studies observed an increased deposit formation with a decrease in temperature difference, CFD studies have always shown a decrease in the crude oil fouling with lower temperature difference between the bulk-fluid and the wall. The effect of bulk temperature at constant wall temperature on coke deposition in a horizontal tube has been studied and observed that the coke deposition on the heat transfer surfaces decreases with an increase in the bulk temperature [24].

Computational fluid dynamics studies offered cost-effective investigations for understanding the crude oil fouling phenomena of crude oils on the heat transfer surfaces. The effects of operating conditions such as flow velocity, temperature difference, etc., have received relatively high attention in the literature. The susceptible locations of deposit formations and the transportation behavior of asphaltene particles in the heat exchanger have received less attention which led to the lack of understanding of non-uniform fouling in the heat exchangers.

3. CFD modeling of asphaltenes deposition in a heat exchanger tube

The behavior of the asphaltene particles is studied in a three-dimensional heat exchanger tube, the geometry, and mesh of which are shown in **Figure 1**. The heat exchanger tube CFD model is developed with a tube length and diameter of 500 and 25 mm, respectively. The asphaltene

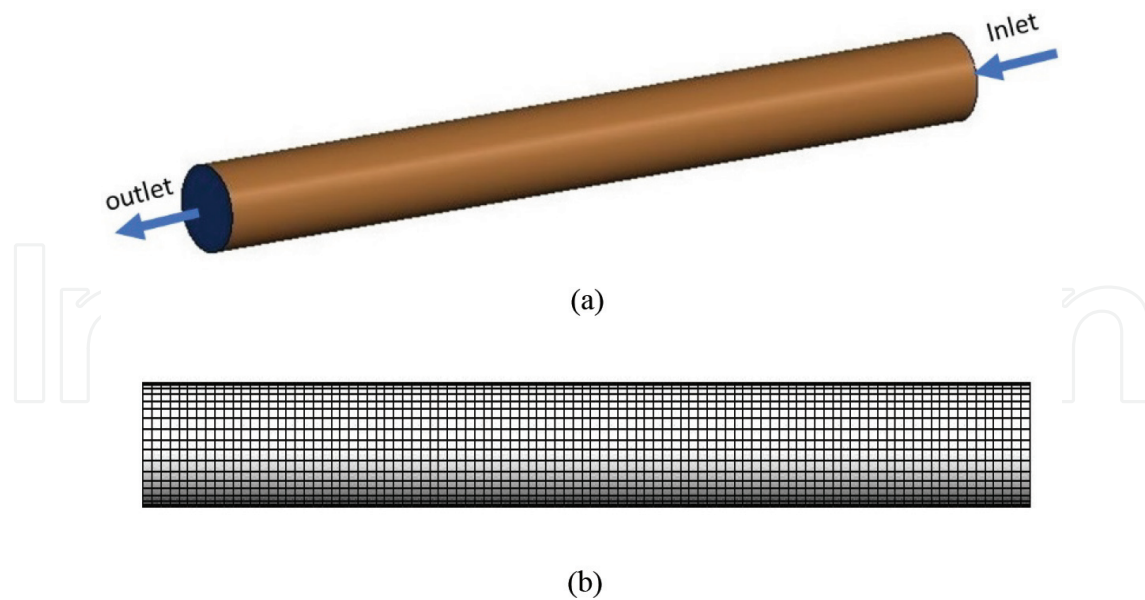


Figure 1: Heat exchanger tube (a) Geometry and (b) grid.

particles' behavior in the heat exchanger tube is studied through a Lagrangian-based DPM mathematical tool available in the commercial CFD software ANSYS FLUENT™ [48]. Discrete phase models are highly used in calculating the trajectories and velocities of particles inside the domain. The effects of various particle sizes on the particle flow paths and the effects of several attractive and repulsive forces on the particles can be predicted through DPM. The particles are considered as discrete phase which interacts with the primary phase. Over the past decades, DPM has been widely used in simulating dilute particle flows, particle deposition analysis, particle dispersion analysis, and vaporization and boiling of particles [49–52]. The influence of the particles on the primary phase is evaluated by momentum exchange fields which are based on the increase or decrease in the particle momentum. These models are generally applicable in situations where the particle volume fraction is less than 12%. Based on the primary phase, the individual particles are traced through various forces acting on it. The particle distribution profiles obtained through DPM and Eulerian-Eulerian simulations are compared and observed that, the DPM simulations provides a better understanding than the Eulerian approach [39].

The described governing equations (Eqs. (1)–(5)) and the appropriate forces (Eqs. (8)–(14)) are considered on the asphaltene particles. Discrete phase-CFD simulation requires a high computational power to expound the particles behavior. Therefore, simulations were performed by activating the enhanced wall treatment effects with k - ϵ turbulence model. The domain is discretized with 0.15 million quadrilateral cells and mesh independence test was performed to validate the consistency and accuracy of the simulation results.

Crude oil has been described as the bulk fluid and asphaltenes are described as discrete phase particles. As asphaltenes have the tendency to aggregate in an irreversible fashion with different particle diameters, the transportation of asphaltenes is modeled with various particles

sizes. The asphaltene particles are injected from inlet surface in the heat exchanger. The properties of the asphaltene particles, boundaries, and operating conditions are given in **Table 1**. The correlations of crude oil properties used in this study are as follows:

Density:

$$\rho = 998.2 \times \left[\frac{((T_b \times 0.154) - 519.11)^{0.5}}{1070.19} \right] \quad (18)$$

Specific heat:

$$C_p = 3980.5 \times [0.4372 + (T_b \times 0.001011)] \quad (19)$$

Thermal conductivity:

$$k = 0.145 - 0.0001T_b \quad (20)$$

In the present simulation, discrete phase particle tracking method has been considered with forces such as gravity, drag, Saffman lift, thermophoretic, and stochastic collision acting on the particles. Initially, a dynamic simulation was performed without activation of the discrete phase models. Once the fully developed flow is observed in the domain, DPM was activated to study the stick, rebound, and splash events of the asphaltene particles as shown in **Figure 2**.

Once the heat exchanger geometry and mesh are developed, the operating and boundary conditions are specified for mesh dependence study. The chosen mesh was used to perform the non-asphaltenes flow simulation with crude oil as medium. The simulation is iterated till the desired convergence with an error tolerance of 1×10^{-6} is achieved. Then, the asphaltene

| Description | Value |
|----------------------|--|
| Density | 1200 kg·m ⁻³ |
| Thermal conductivity | 0.756 W·m ⁻¹ ·K ⁻¹ |
| Heat capacity | 1500 J·kg ⁻¹ ·K ⁻¹ |
| Particle diameter | 0.005–0.1 mm |
| Inlet | Velocity inlet |
| Wall | Wall with no-slip condition |
| Outlet | Outflow |
| Flow velocity | 0.5–1.5 m/s |
| Bulk temperature | 333 K |
| Wall temperature | 375 K |

Table 1. Asphaltene particles' properties, boundaries, and operating conditions.

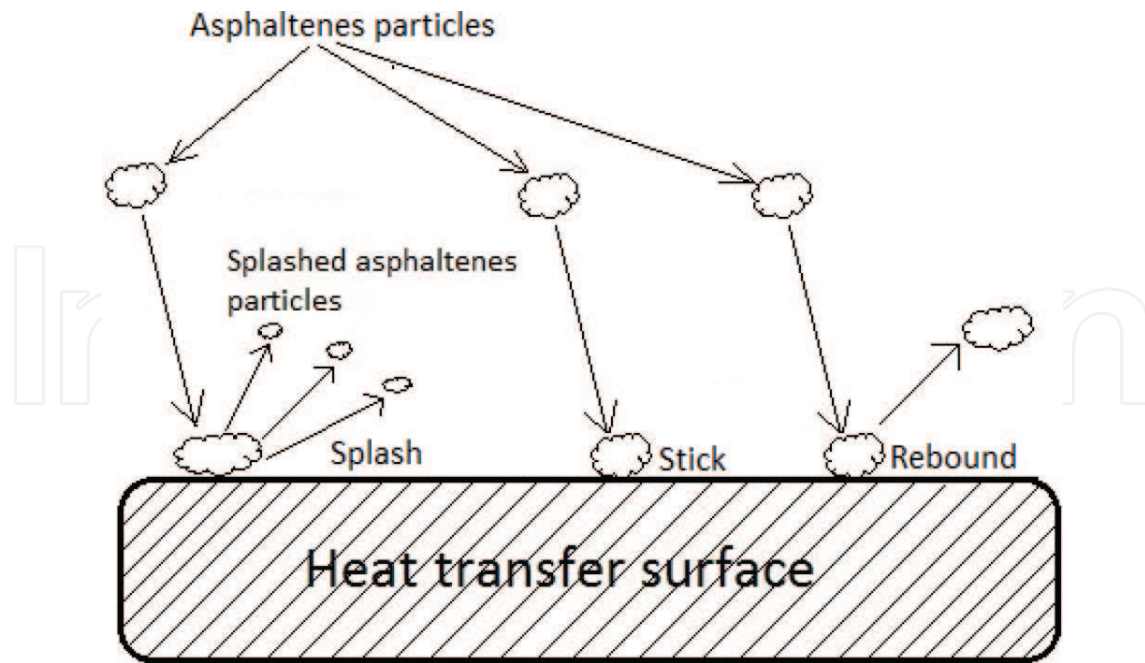


Figure 2. Particle events on the heat transfer surface.

particles are injected into the domain from inlet and their trajectories are investigated with the DPM. As asphaltene particles are physically adhered to the heat transfer surface, a particle based Lagrangian frame approach is employed to understand the transportation and adhesion behavior of asphaltene particles in the heat exchanger. The simulation methodology followed in this study is shown in flow chart in **Figure 3**.

The CFD simulations investigated the transportation and adhesion behavior of asphaltene particles in the heat exchanger tube. The stick, rebound and splash behavior of the asphaltene particles were studied from the discrete phase CFD simulations. From the results obtained, asphaltene mass deposition and deposition film thickness are estimated, which are shown in **Figures 4–6**.

The foulant layer spreading of deposited asphaltene particles is observed from **Figure 4**. Due to the force of gravity, asphaltene particles are deposited on the bottom portion of the tube. **Figures 5** and **6** shows the graphical representation of asphaltene mass deposition and deposition film thickness at various crude oil velocities. It is observed that, at low fluid velocity conditions, asphaltene particles will have a higher mass deposition and deposition film thickness compared with the high fluid velocity conditions.

A three-dimensional CFD study was performed to predict the asphaltene mass deposition from crude oil on the heat transfer surface. From the results obtained, fluid velocity is observed to have a high impact on mitigation of fouling. The discrete phase CFD simulation results clearly forecasts the asphaltene particles deposition locations in the tube, deposition mass, and

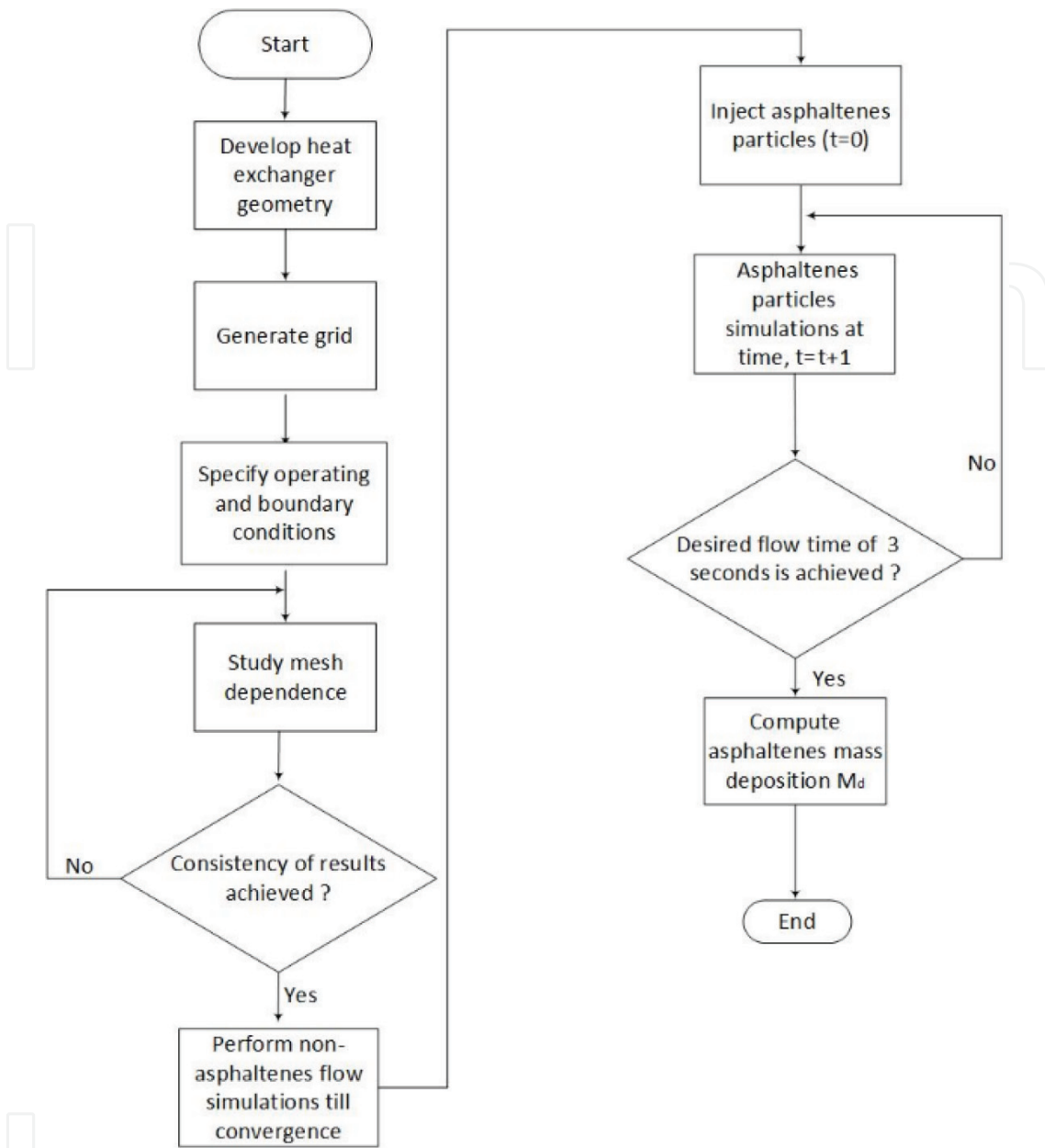


Figure 3. Flow chart—simulation methodology.

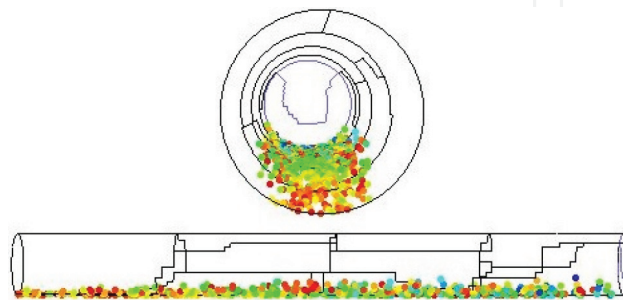


Figure 4. Asphaltene particles' deposition.

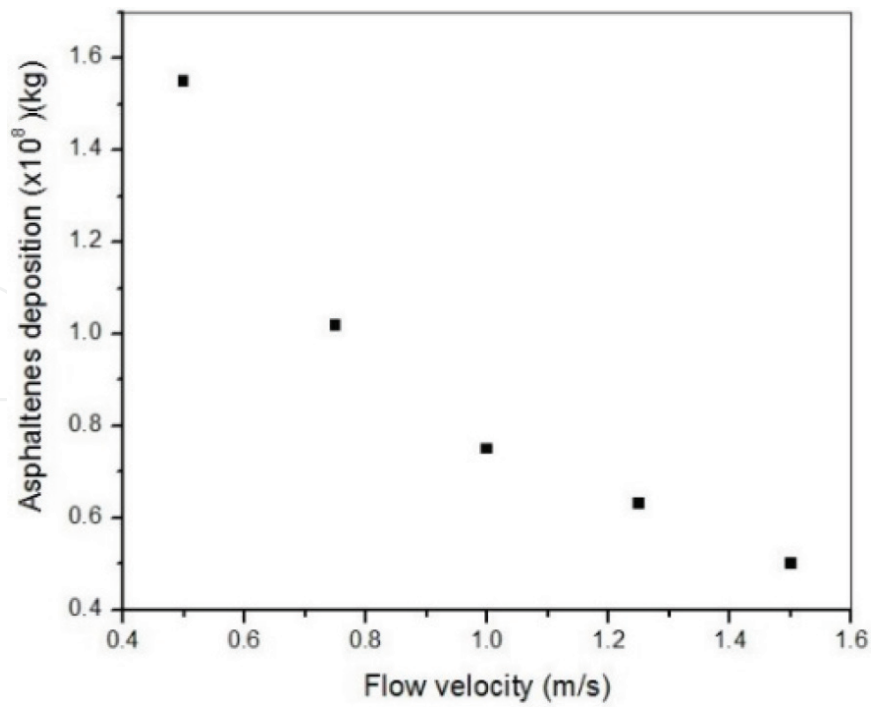


Figure 5. Asphaltene particles' mass deposition vs. flow velocity.

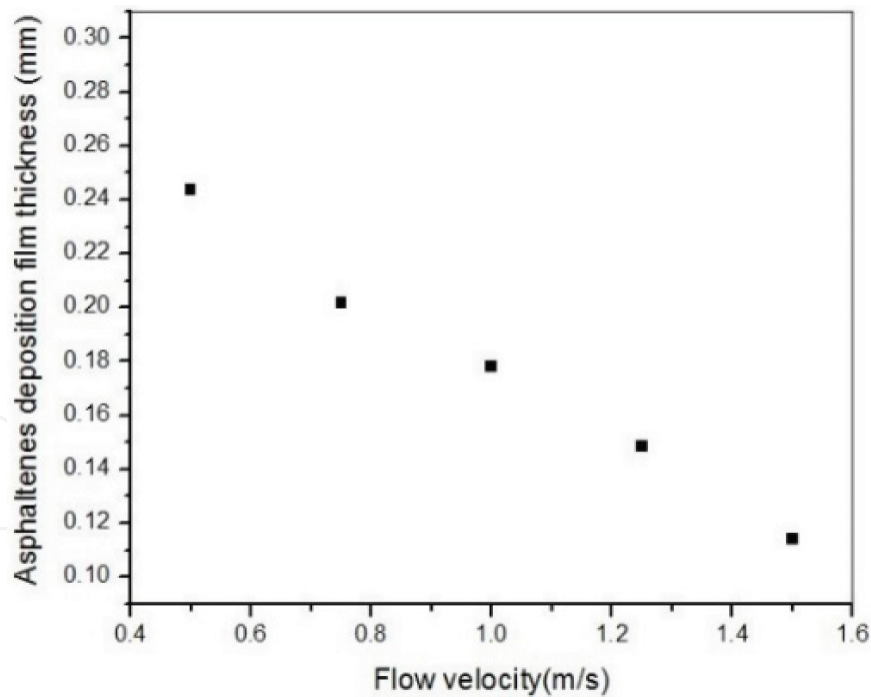


Figure 6. Asphaltene particles' deposition film thickness vs. flow velocity.

deposition film thickness. Therefore, the non-symmetric fouling behavior of crude oil can be modeled using the available CFD techniques, through which the susceptible regions of concern can be predicted in the shell and tube heat exchangers.

4. Conclusions

Although, the fouling phenomena of crude oils are highly complex, the application of CFD simulations offered a high understanding of the fouling process on the heat transfer surfaces. The discrete phase CFD simulation results clearly forecasts the asphaltene particles deposition locations in the tube, deposition mass, and deposition film thickness. The fluid velocity is observed to have a high impact on mitigation of fouling. More research is required to understand the fluid flow behavior of crude oil in the shell and tube heat exchangers. Therefore, the future of CFD in crude oil fouling research is to investigate the flow paths and susceptible regions of crude oil fouling in the heat exchangers.

Nomenclature

| | |
|------------------|---|
| A | pre-exponent factor (1·s) |
| C_1 | empirical constant, 1.44 |
| C_2 | empirical constant, 1.92 |
| C_A | asphaltenes concentration, $\text{kg}\cdot\text{m}^{-3}$ |
| $C_A C_D$ | drag coefficient |
| C_p | concentration of the precursor, $\text{kg}\cdot\text{m}^{-3}$ |
| C_{r1}, C_{r2} | concentration of the reactants, $\text{kg}\cdot\text{m}^{-3}$ |
| C_A | diffusion coefficient, $\text{m}^2\cdot\text{s}$ |
| $C_A d_{ij}$ | deformation tensors |
| $D_{T,p}$ | thermophoretic force coefficient |
| E | activation energy, $\text{J}\cdot\text{mol}^{-1}$ |
| C_A | drag force, N |
| $C_A F_i$ | additional force acting on the particle |
| F_{th} | thermophoretic force |
| $C_A \bar{g}$ | gravitational force, $\text{m}\cdot\text{s}^{-2}$ |
| H | energy source term |
| J | mass flux from the oil-phase to fouling phase, $\text{mol}\cdot\text{m}^{-2}\cdot\text{s}^{-1}$ |
| K | equilibrium constant |
| k | thermal conductivity, $\text{W}\cdot\text{m}^{-1}\cdot\text{K}^{-1}$ in Eq. (3), turbulent kinetic energy, $\text{J}\cdot\text{kg}^{-1}$ in Eq. (4) |
| C_A | reaction rate constant |
| Kn | Knudsen number |

| | |
|--------|--|
| L_x | number of moles present for each phase |
| m, n | orders of reactants and precursors |
| m_p | particle mass, kg |
| m_d | mass deposition rate, $\text{kg}\cdot\text{m}^{-2}\cdot\text{s}^{-1}$ |
| n | the normal vector on the tube walls |
| P | shear production of turbulence, $\text{Pa}\cdot\text{s}$ |
| R | rate of production of species in Eq. (7), universal gas constant, $\text{J}\cdot\text{mol}^{-1}\cdot\text{K}^{-1}$ in Eq. (17) R |
| Re | Reynolds number |
| S | rate of creation |
| T | temperature, K |
| v | fluid velocity, $\text{m}\cdot\text{s}^{-1}$ |

Greek letters

| | |
|----------------------|---|
| τ | shear stress, Pa |
| θ | parameter that depends on L_x |
| ρ | density, $\text{kg}\cdot\text{m}^{-3}$ |
| γ | mass fraction of species |
| η | dimensionless function |
| ΔH | precipitation enthalpy |
| μ | fluid viscosity, $\text{kg}\cdot\text{m}^{-1}\cdot\text{s}^{-1}$ |
| ω | specific turbulence dissipation rate, $\text{J}\cdot\text{kg}^{-1}\cdot\text{s}^{-1}$ |
| ε | turbulence dissipation rate, $\text{J}\cdot\text{kg}^{-1}\cdot\text{s}^{-1}$ |
| σ_k | empirical constant, 1.00 |
| σ_ε | empirical constant, 1.30 |

Subscripts

| | |
|-----|-------------|
| A | asphaltenes |
| b | bulk |
| w | wall |

s surface

p particle

p, q phase

Author details

Ramasamy Marappa Gounder* and Sampath Emani

*Address all correspondence to: marappagounder@utp.edu.my

Department of Chemical Engineering, Universiti Teknologi PETRONAS, Seri Iskandar, Perak D.R., Malaysia

References

- [1] Müller-Steinhagen H, Malayeri M, Watkinson A. Heat exchanger fouling: Environmental impacts. *Heat Transfer Engineering*. 2009;**30**:773-776
- [2] Wiehe I. Petroleum fouling: Causes, tools and mitigation methods. In: *Proceedings of the 9th Topical Conference on Refinery Processing*; 2006
- [3] Hasson D. *Precipitation Fouling*. New York: Hemisphere Publishing Corp; 1981. pp. 527-568
- [4] Watkinson AP, Panchal C. *A Critical Review of Organic Fluid Fouling*. IL, USA: Argonne National Lab; 1990
- [5] Watkinson A, Wilson D. Chemical reaction fouling: A review. *Experimental Thermal and Fluid Science*. 1997;**14**:361-374
- [6] Awad M. Fouling of Heat Transfer Surfaces, *Heat Transfer—Theoretical Analysis, Experimental Investigations and Industrial Systems*. Croatia: InTech; 2011: 506-542. ISBN: 978-953-307-226-5
- [7] Kent C. Biological fouling: Basic science and models. In: *Fouling Science and Technology*. Dordrecht: Springer; 1988. pp. 207-222
- [8] Shetty N, Deshannavar UB, Marappagounder R, Pendyala R. Improved threshold fouling models for crude oils. *Energy*. 2016;**111**:453-467
- [9] Knudsen J, Lin D, Ebert W. The determination of the threshold fouling curve for a crude oil. In: *Understanding Heat Exchanger Fouling and Its Mitigation*. Proceedings of an International Conference on Understanding Heat Exchanger Fouling and Its Mitigation, Begell House, New York, 1999. pp. 265-272. ISBN: 156700136X 9781567001365

- [10] Polley GT, Wilson D, Yeap B, Pugh S. Evaluation of laboratory crude oil threshold fouling data for application to refinery pre-heat trains. *Applied Thermal Engineering*. 2002;**22**: 777-788
- [11] Panchal C, Kuru W, Liao C, Ebert W, Palen J. Threshold conditions for crude oil fouling. In: *Understanding Heat Exchanger Fouling and Its Mitigation*. Proceedings of an International Conference on Understanding Heat Exchanger Fouling and Its Mitigation, Begell House, New York, 1999. pp: 273-282. ISBN: 156700136X 9781567001365
- [12] Kern D, Seaton R. A theoretical analysis of thermal surface fouling. *British Chemical Engineering*. 1959;**4**:258-262
- [13] Emani S, Ramasamy M, Shaari KZBK. Effect of shear stress on crude oil fouling in a heat exchanger tube through CFD simulations. *Procedia Engineering*. 2016;**148**:1058-1065
- [14] Bayat M, Aminian J, Bazmi M, Shahhosseini S, Sharifi K. CFD modeling of fouling in crude oil pre-heaters. *Energy Conversion and Management*. 2012;**64**:344-350
- [15] Sileri D, Sahu K, Ding H, Matar O. Mathematical modelling of asphaltene deposition and removal in crude distillation units. In: *International Conference on Heat Exchanger Fouling and Cleaning VIII*. Schlading Austria; 2009. pp. 245-251
- [16] Haghshenasfard M, Hooman K. CFD modeling of asphaltene deposition rate from crude oil. *Journal of Petroleum Science and Engineering*. 2015;**128**:24-32
- [17] Mukherjee R. Effectively design shell-and-tube heat exchangers. *Chemical Engineering Progress*. 1998;**94**:21-37
- [18] Jatale A, Srinivasa M. CFD Modeling of Fouling in Crude Oil Refinery Heat Exchangers. Spring Meeting and 11th Global Congress on Process Safety-AIChE, Austin, 2015
- [19] Wang Y, Lu Q, Zheng Y, Yuan B, Tao H. A CFD-based analysis on trends of heat exchanger fouling. In: *2012 Asia-Pacific Power and Energy Engineering Conference*. IEEE; 2012. pp. 1-4
- [20] Clarke R, Nicolas F. CFD investigation of maldistribution effects on crude oil fouling in shell and tube exchangers. In: *Second International Conference on Petroleum and Gas Phase Behaviour and Fouling*. Copenhagen, Denmark; 2000
- [21] Anderson JD, Wendt J. *Computational Fluid Dynamics*. Heidelberg: Springer; 1995
- [22] Tu J, Yeoh GH, Liu C. *Computational Fluid Dynamics: A Practical Approach*. Oxford: Butterworth-Heinemann; 2012
- [23] Sun D-W. *Computational Fluid Dynamics in Food Processing*. Boca Raton: CRC Press; 2007. ISBN: 9780849392863
- [24] Li X-G, Zhang L-H, Zhang R-Y, Sun Y-L, Jiang B, Luo M-F, Li X-G. CFD modeling of phase change and coke formation in petroleum refining heaters. *Fuel Processing Technology*. 2015;**134**:18-25

- [25] Nazar S, Ali R, Banisharifdehkordi F, Ahmadzadeh S. Mathematical modeling of coke formation and deposition due to thermal cracking of petroleum fluids. *Chemical Engineering & Technology*. 2016;**39**:311-321
- [26] Fontoura D, Matos E, Nunhez J. A three-dimensional two-phase flow model with phase change inside a tube of petrochemical pre-heaters. *Fuel*. 2013;**110**:196-203
- [27] Souza B, Matos E, Guirardello R, Nunhez J. Predicting coke formation due to thermal cracking inside tubes of petrochemical fired heaters using a fast CFD formulation. *Journal of Petroleum Science and Engineering*. 2006;**51**:138-148
- [28] Fouzia D, Park TS. Effect of inlet velocity on the crude oil coking and gas phase formation in a straight pipe. *Journal of Applied Mathematics and Physics*. 2016;**5**:17
- [29] Seyyedbagheri H, Mirzayi B. CFD modeling of high inertia asphaltene aggregates deposition in 3D turbulent oil production wells. *Journal of Petroleum Science and Engineering*; 2016
- [30] Wilcox DC. *Turbulence Modeling for CFD*. 3rd ed. LA: D.C.W. Industries, Inc.; 2006
- [31] Yang J, Serratos MGJ, Fari-Arole DS, Müller EA, Matar OK. Crude oil fouling: Fluid dynamics, reactions and phase change. *Procedia IUTAM*. 2015;**15**:186-193
- [32] Coletti F, Hewitt G. *Crude Oil Fouling*. Elsevier, USA: Gulf Professional Publishing; 2015
- [33] Jamialahmadi M, Soltani B, Müller-Steinhagen H, Rashtchian D. Measurement and prediction of the rate of deposition of flocculated asphaltene particles from oil. *International Journal of Heat and Mass Transfer*. 2009;**52**:4624-4634
- [34] Daaou M, Larbi A, Martínez-Haya B, Rogalski M. A comparative study of the chemical structure of asphaltenes from Algerian petroleum collected at different stages of extraction and processing. *Journal of Petroleum Science and Engineering*. 2016;**138**:50-56
- [35] Ge Q, Yap Y, Vargas F, Zhang M, Chai J. Numerical modeling of asphaltene deposition. *Computational Thermal Sciences*. 2013;**5**:153-163
- [36] Miri R, Zendeboudi S, Kord S, Vargas F, Lohi A, Elkamel A, Chatzis I. Experimental and numerical modeling study of gravity drainage considering asphaltene deposition. *Industrial & Engineering Chemistry Research*. 2014;**53**:11512-11526
- [37] Mirzayi B, Mousavi Dehghani SA, Chakan MB. Modeling of asphaltene deposition in pipelines. *Journal of Petroleum Science and Technology*. 2013;**3**:15-23
- [38] Zhu H, Jing J, Li Q, Yu X, Junwen C. Simulations of asphaltene deposition in submarine pipelines by CFD. In: *International Oil and Gas Conference and Exhibition in China*. Society of Petroleum Engineers; 2010
- [39] Zhang Z, Chen Q. Comparison of the Eulerian and Lagrangian methods for predicting particle transport in enclosed spaces. *Atmospheric Environment*. 2007;**41**:5236-5248

- [40] Al-Fulaij H, Cipollina A, Micale G, Ettouney H, Bogle D. Eulerian–Lagrangian modeling and computational fluid dynamics simulation of wire mesh demisters in MSF plants. *Desalination*. 2016;**385**:148-157
- [41] Cokljat D, Slack M, Vasquez S, Bakker A, Montante G. Reynolds-stress model for Eulerian multiphase. *Progress in Computational Fluid Dynamics, An International Journal*. 2006; **6**:168-178
- [42] Kohse BF, Nghiem LX. Modelling asphaltene precipitation and deposition in a compositional reservoir simulator. In: *SPE/DOE Symposium on Improved Oil Recovery*. Society of Petroleum Engineers; 2004
- [43] Behbahani TJ, Behbahani ZJ. A new study on asphaltene adsorption in porous media. *Petroleum and Coal*. 2014;**56**:459-466
- [44] Talbot L, Cheng R, Schefer R, Willis D. Thermophoresis of particles in a heated boundary layer. *Journal of Fluid Mechanics*. 1980;**101**:737-758
- [45] Saffman P. The lift on a small sphere in a slow shear flow. *Journal of Fluid Mechanics*. 1965;**22**:385-400
- [46] Mahulkar AV, Heynderickx GJ, Marin GB, Varbanov P, Lam H, Klemes J, Pierucci S. Simulation of coking in convection section of steam cracker. *Chemical Engineering*. 2012;**29**
- [47] Brahim F, Augustin W, Bohnet M. Numerical simulation of the fouling process. *International Journal of Thermal Sciences*. 2003;**42**:323-334
- [48] <http://www.ansys.com/Products/Fluids/ANSYS-Fluent>
- [49] Emani S, Ramasamy M, Ki Zilati KS. CFD modelling of shell-side asphaltene deposition in a shell and tube heat exchanger. *American Institute of Physics*. 2017;**1859**:020118-1-020118-7
- [50] Emani S, Ramasamy M, Ki Zilati KS. Transportation and adhesion of asphaltene in a heat exchanger tube through CFD simulations. *American Institute of Physics*. 2017;**1859**:020119-1-020119-7
- [51] Pirker S, Kahrmanovic D, Goniva C. Improving the applicability of discrete phase simulations by smoothening their exchange fields. *Applied Mathematical Modelling*. 2011;**35**:2479-2488
- [52] Subhasish M, Mayur JS, Elham D, Geoffrey ME. Investigation of droplet evaporation in a bubbling fluidized bed. In: *Ninth International Conference on CFD in the Minerals and Process Industries*. CSIRO; Melbourne, Australia; 2012

